applied optics

Characterization of a single-frequency bismuth-doped fiber power amplifier with a continuous wave and modulated seed source at 1687 nm

Grzegorz Gomolka,[1,4] Aleksandr M. Khegai,[2] Sergei V. Alyshev,[2] Aleksey S. Lobanov,[3] Sergei V. Firstov,[2] and Michal Nikodem[1,*]

[1]Department of Optics and Photonics, Wroclaw University of Science and Technology, Wybrzeze Wyspianskiego 27, 50-370 Wroclaw, Poland
[2]Fiber Optics Research Center, Russian Academy of Sciences, 38 Vavilova, 119333 Moscow, Russia
[3]Institute of Chemistry of High Purity Substances, Russian Academy of Sciences, 29 Tropinina, 603600 Nizhny Novgorod, Russia
[4]e-mail: grzegorz.gomolka@pwr.edu.pl
*Corresponding author: michal.nikodem@pwr.edu.pl

Received 26 November 2019; revised 9 January 2020; accepted 9 January 2020; posted 10 January 2020 (Doc. ID 384413); published 12 February 2020

In this paper, we report the performance of a bismuth-doped fiber amplifier at 1687 nm. This wavelength region is particularly interesting for laser-based spectroscopy and trace gas detection. The active bismuth-doped fiber is pumped at 1550 nm. With less than 10 mW of the seed power, more than 100 mW is obtained at the amplifier's output. We also investigate the signal at the output when a wavelength-modulated seed source is used, and present wavelength modulation spectroscopy of methane transition near 1687 nm. A significant baseline is observed in the spectra recorded when the fiber amplifier is used. The origin of this unwanted background signal is discussed and methods for its suppression are demonstrated.

https://doi.org/10.1364/AO.384413

1. INTRODUCTION

Molecular spectroscopy in the infrared spectral region plays an important role in numerous applications, from environmental monitoring to gas leak detection. Various near- and mid-infrared optical sources are used in laser-based spectroscopy, including, e.g., optical frequency combs for broadband measurements [1,2] or pulsed sources (based on optical parametric oscillators [3] or solid-state devices such as Er:YAG lasers [4]) for differential absorption LIDAR (DIAL). However, highly sensitive optical-based gas-sensing applications usually rely on compact and narrow-linewidth single-frequency laser diodes (for wavelengths below ~ 3 μm) or interband/quantum cascade lasers (for wavelengths longer than ~ 3 μm). In optical-based gas detection, the near-infrared region (compared to the mid-infrared) offers weaker molecular transitions but also less expensive lasers and detectors, and a variety of fiber-based components. Additionally, in many cases, one can use optical fiber amplifiers to increase the optical power emitted from single-frequency laser diodes. For example, it was demonstrated that erbium-doped fiber amplifiers (EDFAs) may be used to improve the performance of quartz-enhanced photoacoustic spectroscopy (QEPAS) [5–7] or extend the measurement range in stand-off detection using wavelength modulation spectroscopy (WMS) [8,9]. Unfortunately, the gain bandwidth of EDFAs is limited to 1525–1620 nm, and they cannot be effectively used at longer wavelengths where various molecules have their rovibrational transitions, including methane (some useful absorption lines are near 1645 nm [10], 1651 nm [11–13], 1653 nm [14–16], 1666 nm [17], or 1674 nm [18]), ethane (near 1684 nm) [14,19], or acetone (near 1690 nm) [20].

Raman amplifiers may be used to obtain gain beyond 1620 nm. However, although they can provide high output powers [21], they also have several drawbacks. For example, Raman amplifiers require use of a very long fiber (up to few kilometers), which often leads to problems with stimulated Brillouin scattering. They also must be pumped at properly chosen wavelengths and have relatively narrow gain bandwidth. Thulium-doped fiber amplifiers may also be used for wavelengths below 1700 nm [22]. Unfortunately, their saturation power in this spectral region is limited, e.g., output power of less than 50 mW was recently demonstrated in [23]. As we have demonstrated in our previous work, higher output powers may

be achieved with bismuth-doped fiber (BDF) [24]. BDF-based amplifiers (BDFAs) can be used to provide gain between 1150 and 1450 nm [25–28] and, more importantly, from 1600 to 1800 nm [29,30]. This makes BDFAs potentially an interesting tool in some gas-sensing applications, including photoacoustic spectroscopy or remote detection of leaks.

In this paper, we analyze the performance of a BDFA at 1687 nm, where we target the P(6) transition in the $2\upsilon_3$ band of methane. This absorption line is well isolated from other atmosphere compounds such as water vapor or carbon dioxide, making it suitable for open-path methane sensing even with very long optical paths (e.g., hundreds of meters and more). In the first part of this paper, the impact of the pump power on the output power is analyzed using a continuous wave (CW) seed source. In the second part, we investigate the performance of the amplifier with a current-modulated seed laser diode. Spectroscopy of methane is demonstrated and the impact of the BDFA on the residual amplitude modulation (RAM) is discussed.

2. EXPERIMENTAL SETUP

The experimental setup is presented in Fig. 1. The active fiber was pumped at 1550 nm using a distributed feedback (DFB) laser diode (output power of approximately 10 dBm) amplified with an erbium/ytterbium-doped fiber amplifier (EYDFA; BKtel, model GOA-S320, maximum output power 32 dBm). The output power of the EYDFA was controlled using a computer. The BDF used in this work was previously introduced in [24]; it has a step-index refractive index profile (0.06 difference between the core and the cladding), core diameter of 2.2 μm, and cut-off wavelength near 1.4 μm. BDF length was selected to make sure that most of the pump power will be absorbed and the entire fiber will be pumped. With Bi concentration below 0.1 mol.%, this resulted in a 90 m long piece of fiber (approximately 95% of absorption at 1550 nm). As in our previous work [24], the pump light and amplifier output signal were coupled in and out of the BDF using a broadband optical circulator. Its transmission at 1687 nm was measured to be approximately 70%. An additional fiber-based isolator was placed between the BDF and the seed laser to block all unabsorbed pump light. The seed laser was a discrete mode (DM) laser diode (from Eblana Photonics) which was driven using a compact laser driver integrated with a temperature controller (from Wavelength Electronics, model LDTC0520). A power meter (from Thorlabs, model PM100D with S132C sensor) was used to measure the output power.

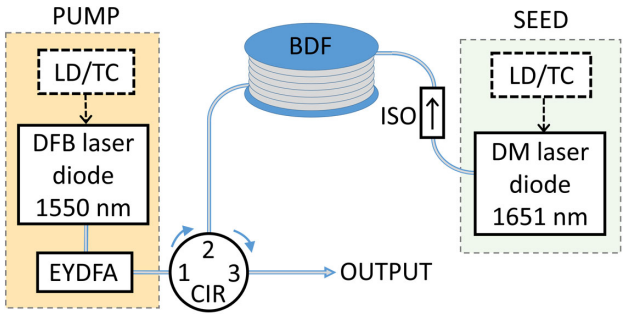

Fig. 1. Schematic diagram of the experimental setup (ISO, optical isolator; CIR, optical circulator; LD/TC, laser driver with temperature controller).

3. EXPERIMENTAL RESULTS

A. BDFA Output Power

Figure 2(a) shows how the output power of the amplifier depends on the pump power with 7.67 mW emitted from the seed laser. As the pump power was gradually increased from 16 dBm (∼ 40 mW) to 29 dBm (∼ 795 mW), a linear increase of the output power was observed. For the highest pumping power, 107 mW at 1687 nm was measured at the output. This corresponds to a gain of approximately 11.4 dB and an efficiency of ∼ 13.5%. As shown in Fig. 2(b), the output power becomes saturated at the input power of approximately 5 mW.

For higher pumping powers, the performance of the amplifier was impeded by the stimulated Brillouin scattering (SBS) that occurred inside BDF. The presence of SBS was confirmed by measuring the output spectra near 1550 nm for different pumping powers (shown in Fig. 3). Two signals are visible; the first one is near 1549.95 nm, and its amplitude is proportional to the pumping power level. The presence of this signal may be explained, e.g., by the back-reflections of the pump radiation from the splice between the BDF and circulator. The second signal is near 1550.02 nm; it is barely visible for low pumping powers, but its amplitude dramatically increases when the pump power exceeds ∼ 700 mW. This nonlinear power dependence as well as frequency shift with respect to the pump wavelength are typical for SBS [31], and were also observed in our previous studies for similar pump power levels [24].

B. BDFA Output with a Modulated Seed Source

As mentioned earlier, one potential application of fiber amplifiers may be standoff gas detection in which a laser beam is sent

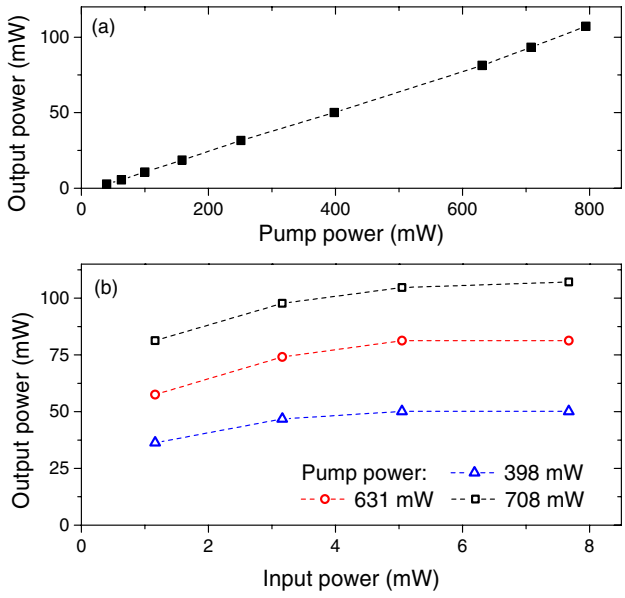

Fig. 2. (a) Output power versus pump power measured for the seed laser power of 7.67 mW; (b) output power versus input (seed laser) power for different pump powers.

towards some topographic target, the back-scattered light is measured, and appropriate signal processing is used to retrieve information about molecular absorption in the laser's path. This type of detection typically uses the WMS technique, in which the laser diode is wavelength-modulated at frequency f_m. Subsequently, the signal from the photodetector is recorded and its component at $2 \times f_m$ is retrieved, usually using lock-in (phase sensitive) detection [32,33]. When the absorption at the molecular transition center is less than ~ 10%, the amplitude of this second-harmonic signal is proportional to both molecular concentration and optical power that reaches the detector. Usually, in order to remove the dependence on the optical power level, the average optical power is also measured (by detecting a DC or $1 \times f_m$ component of the signal from the detector), and it is used to normalize the $2f$ WMS signal. Consequently, a power-normalized $2f$ WMS signal (often called $2f/1f$ WMS) is obtained and its amplitude depends only on molecular concentration [34]. Power normalization with a $1 \times f_m$ component is sometimes preferable because it allows use of an AC coupled detector.

Wavelength modulation required for WMS is typically achieved through current modulation of the laser diode. The additional ramp signal is also often used in order to record the full $2f$ WMS spectrum [35]. Unfortunately, changes to the driving current not only affect the wavelength emitted from the laser but also its output power. The output power versus laser current characteristic of the laser diode used in this work is shown in Fig. 4(a), and is almost linear; thus, the power modulation at its output is basically a replica of the current modulation. However, as shown in Fig. 2(b) and (in more detail) in Fig. 4(a), the output power dependence of a BDFA on its input power is not linear. As a result, the power modulation at the output of the amplifier will change as the laser diode's wavelength is tuned [as shown schematically in Fig. 4(a) and experimentally in Fig. 4(b)], affecting both harmonics (first and second) typically used for WMS measurements.

To demonstrate this effect, the output of the amplifier was passed through a 10 cm long glass cell containing methane (at the concentration of 5%, balanced with nitrogen) placed between two GRIN collimators and focused onto the detector (Thorlabs, model PDA10CS2). A Virtual Bench device (National Instruments) was used to modulate the seed laser's current with a 2.5 kHz sinusoid (15 mA peak–peak) and an additional ramp signal for wavelength scanning (from 25 to 87.5 mA). The same instrument was used to acquire the signal from the photodetector. The lock-in (phase-sensitive) detection of the second-harmonic WMS signal was performed using a custom LabVIEW program.

Figure 5 presents the $2f$ WMS spectra acquired without and with amplifier (at two different pumping powers). When only laser diode is used (without BDFA), the obtained spectrum is identical to that simulated using data from HITRAN database (also shown). However, when BDFA is used, a significant baseline appears which results from the nonlinear transfer function of the amplifier.

Because baseline dominates in the lower-input-power part of the spectrum, its impact can be reduced when the injection current and temperature of the seed laser are chosen appropriately. However, when more effective and broadband suppression of the baseline is needed, two approaches may be implemented.

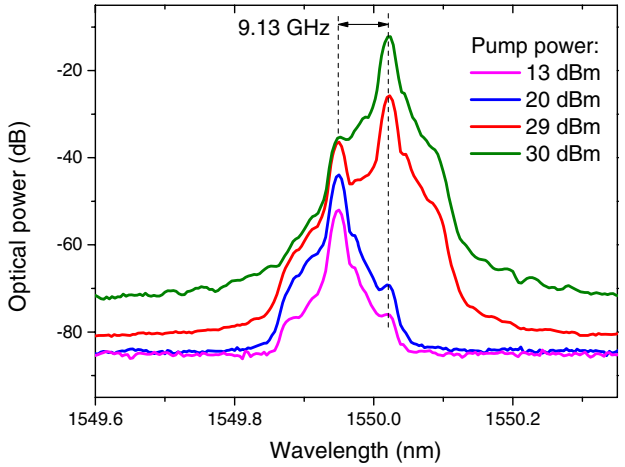

Fig. 3. Optical spectra near 1550 nm for different pump powers. The back-reflected pump signal is visible near 1549.95 nm. For higher pump powers a Stokes wave appears, frequency-shifted by ~ 9.13 GHz (both wavelengths are indicated with dashed lines).

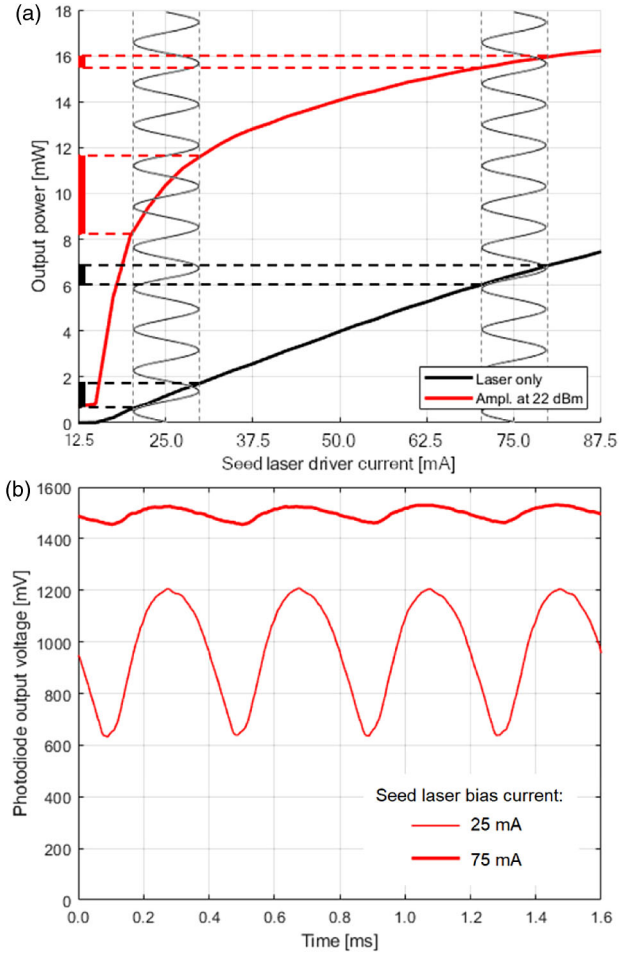

Fig. 4. (a) Output power versus seed laser current for the laser only and laser amplified by BDF (pumped at 22 dBm). It is shown schematically that due to nonlinearities of its transfer function, the fiber amplifier will introduce distortions to the output power modulation. (b) Modulated signals for low and high seed laser bias current, when BDFA is pumped at 22 dBm.

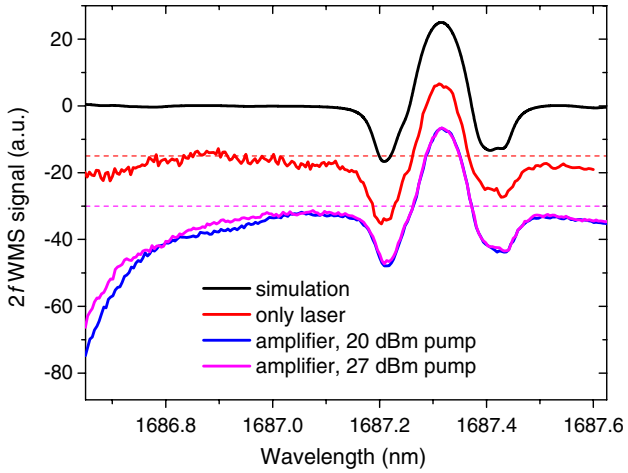

Fig. 5. Comparison between 2 f WMS spectra measured with seed laser only (no amplifier) and with BDFA at 20 and 27 dBm pump power. Also shown is a spectrum simulated using HITRAN database [36]. For viewing purposes, the measured spectra are vertically shifted by −15 and −30 a.u. (dashed lines show "zero" after the shift).

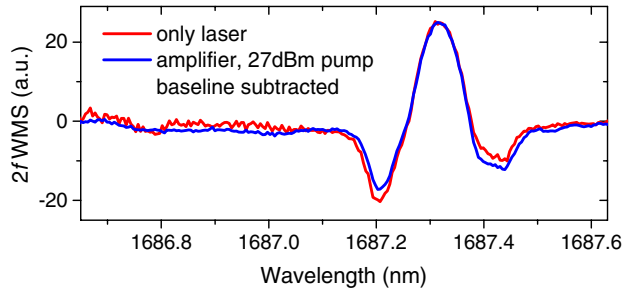

Fig. 6. Second-harmonic signals obtained with the seed laser only and with the amplifier pumped at 27 dBm after subtraction of the baseline.

The first approach involves an additional sensing path (with no gas sample) which may be used to separately record the baseline only. This signal may be subsequently used to subtract the baseline from the original 2 f WMS spectrum. As shown in Fig. 6, this approach may be very effective. Unfortunately, it requires the second photodetector and lock-in amplifier.

The other baseline removal approach relies on the fact that the 2 f WMS signal from the methane sample and the baseline are phase-shifted with respect to each other. As a result, it is possible to adjust the lock-in amplifier phase so that the baseline is removed while the spectroscopic signal is still visible. An example is shown in Fig. 7, where 2 f WMS spectra recorded for two different phase settings are shown. A phase of 2.82 rad provides the maximum signal amplitude but with the baseline present in the background. When the phase is changed to 1.59 rad, the signal amplitude is reduced by approximately 55% but the baseline is not present anymore. This tradeoff may be acceptable in some applications in which accuracy and long-term stability (which may be affected by the baseline drifts) are more important than the detection limit and precision.

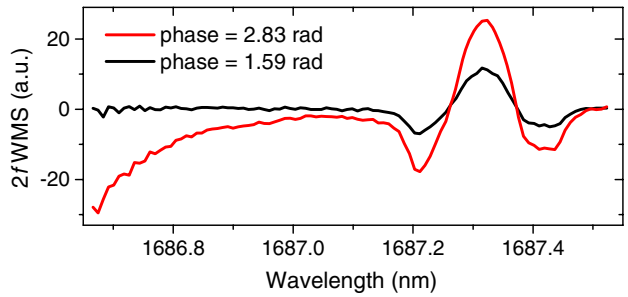

Fig. 7. Second-harmonic signals obtained with BDFA pumped at 28 dBm for two different lock-in amplifier phase settings. The proper choice of the demodulation phase results in baseline-free 2 f WMS spectrum at the price of reduced signal amplitude.

4. CONCLUSIONS

In this paper, the performance of a bismuth-doped fiber power amplifier near 1687 nm was presented and analyzed. An output power of 107 mW was obtained for the input power of 7.7 mW and pump power (at 1550 nm) of almost 800 mW. This is approximately 33% higher output power than reported in [24], where BDFA operation at 1651 nm was analyzed. The performance presented in this paper was primarily limited by the stimulated Brillouin scattering at the pump wavelength and relatively low transmission (∼70%) of the optical circulator used for out-coupling the amplified signal at 1687 nm.

Compared to other potential sources used for methane detection in this spectral region, the presented fiber-amplified source offers several advantages when certain gas-sensing techniques are used. The output power of approximately 100 mW would not be high enough for DIAL measurements (in which pulsed sources with high pulse energies are required [3,4,37]), but it may be very useful in stand-off detection that relies on light backscattered from solid targets [8]. It may also be combined with sensors that use photoacoustic spectroscopy for concentration detection [6,7]. Methane absorption lines near 1.6–1.7 μm are approximately 30 times weaker than the strongest infrared transitions near 3.3 μm. This explains why, in [38], the detection limits of 127 ppb (for 3.5 mW) and 10.7 ppb (for 2 mW) were obtained for the near- and mid-infrared sources, respectively. However, because signal amplitude in photoacoustic spectroscopy scales with optical power [5–7], fiber amplifiers such as those presented in this work should enhance the signal amplitude in the near-infrared QEPAS and improve detection sensitivity, despite the large difference in line strength.

In the second part of the paper, the performance of the amplifier with the current-modulated seed source was analyzed. We have demonstrated that due to nonlinearity of the amplifier's transfer function, the sinusoidal signal is distorted after passing through the amplifier. This distortion affects not only the output signal amplitude but also its harmonic content, resulting in the presence of the baseline when wavelength modulation spectroscopy with the second-harmonic detection is used. Two approaches that enable removing this baseline were experimentally demonstrated. It is also worth mentioning that this issue will not be that critical in techniques which can benefit from higher optical power provided by the amplifier but in which the measured signal amplitude does not rely directly on amplitude modulation (e.g., in chirped laser dispersion spectroscopy [39] or quartz-enhanced photoacoustic spectroscopy).

Funding. Narodowe Centrum Nauki (UMO-2018/29/B/ST7/01730); Ośrodek Przetwarzania Informacji (POIR.04.02.00-00-B003/18); Russian Science Foundation (19-72-10003).

Disclosures. The authors declare no conflicts of interest.

REFERENCES

1. J. Chen, X. Zhao, Z. Yao, T. Li, Q. Li, S. Xie, J. Liu, and Z. Zheng, "Dual-comb spectroscopy of methane based on a free-running Erbium-doped fiber laser," Opt. Express **27**, 11406–11412 (2019).
2. K. C. Cossel, E. M. Waxman, I. A. Finneran, G. A. Blake, J. Ye, and N. R. Newbury, "Gas-phase broadband spectroscopy using active sources: progress, status, and applications [Invited]," J. Opt. Soc. Am. B **34**, 104–129 (2017).
3. T. F. Refaat, S. Ismail, A. R. Nehrir, J. W. Hair, J. H. Crawford, I. Leifer, and T. Shuman, "Performance evaluation of a 1.6 μm methane DIAL system from ground, aircraft and UAV platforms," Opt. Express **21**, 30415–30432 (2013).
4. H. Fritsche, O. Lux, C. Schuett, S. Heinemann, W. Gries, and H. J. Eichler, "Efficient Er:YAG lasers at 1645.55 nm, resonantly pumped with narrow bandwidth diode laser modules at 1532 nm, for methane detection," Proc. SPIE **8599**, 83–89 (2013).
5. Y. He, Y. Ma, Y. Tong, X. Yu, and F. K. Tittel, "HCN ppt-level detection based on a QEPAS sensor with amplified laser and a miniaturized 3D-printed photoacoustic detection channel," Opt. Express **26**, 9666–9675 (2018).
6. H. Wu, L. Dong, X. Liu, H. Zheng, X. Yin, W. Ma, L. Zhang, W. Yin, and S. Jia, "Fiber-amplifier-enhanced QEPAS sensor for simultaneous trace gas detection of NH3 and H2S," Sensors **15**, 26743–26755 (2015).
7. Y. Ma, Y. He, Y. Tong, X. Yu, and F. K. Tittel, "Ppb-level detection of ammonia based on QEPAS using a power amplified laser and a low resonance frequency quartz tuning fork," Opt. Express **25**, 29356–29364 (2017).
8. M. B. Frish, R. T. Wainner, M. C. Laderer, B. D. Green, and M. G. Allen, "Standoff and miniature chemical vapor detectors based on tunable diode laser absorption spectroscopy," IEEE Sens. J. **10**, 639–646 (2010).
9. R. T. Wainner, M. B. Frish, D. Green, M. C. Laderer, M. Allen, and J. Morency, "High altitude aerial natural gas leak detection system," in Final report PSI-1454/TR-2211 (Physical Science Inc., 2006).
10. A. M. Cubillas, M. Silva-Lopez, J. M. Lazaro, O. M. Conde, M. N. Petrovich, and J. M. Lopez-Higuera, "Methane detection at 1670-nm band using a hollow-core photonic bandgap fiber and a multiline algorithm," Opt. Express **15**, 17570–17576 (2007).
11. E. J. Zhang, C. C. Teng, T. G. van Kessel, L. Klein, R. Muralidhar, G. Wysocki, and W. M. J. Green, "Field deployment of a portable optical spectrometer for methane fugitive emissions monitoring on oil and gas well pads," Sensors **19**, 2707 (2019).
12. J. Xia, F. Zhu, S. Zhang, A. Kolomenskii, and H. Schuessler, "A ppb level sensitive sensor for atmospheric methane detection," Infrared Phys. Technol. **86**, 194–201 (2017).
13. M. B. Frish, R. T. Wainner, J. Stafford-Evans, B. D. Green, M. G. Allen, S. Chancey, J. Rutherford, G. Midgley, and P. Wehnert, "Standoff sensing of natural gas leaks: evolution of the remote methane leak detector (RMLD)," in *Conference on Lasers and Electro-Optics/Quantum Electronics and Laser Science and Photonic Applications, Systems and Technologies*, OSA Technical Digest (CD) (Optical Society of America, 2005), paper JThF3.
14. X. Tian, Y. Cao, J. Chen, K. Liu, G. Wang, T. Tan, J. Mei, W. Chen, and X. Gao, "Dual-gas sensor of CH4/C2H6 based on wavelength modulation spectroscopy coupled to a home-made compact dense-pattern multipass cell," Sensors **19**, 820 (2019).
15. K. Liu, L. Wang, T. Tan, G. Wang, W. Zhang, W. Chen, and X. Gao, "Highly sensitive detection of methane by near-infrared laser absorption spectroscopy using a compact dense-pattern multipass cell," Sens. Actuat. B Chem. **220**, 1000–1005 (2015).
16. J. Jiang, Z. Wang, X. Han, C. Zhang, G. Ma, C. Li, and Y. Luo, "Multi-gas detection in power transformer oil based on tunable diode laser absorption spectrum," IEEE Trans. Dielectr. Electr. Insul. **26**, 153–161 (2019).
17. K. Ikuta, N. Yoshikane, N. Vasa, Y. Oki, M. Maeda, M. Uchiumi, Y. Tsumura, J. Nakagawa, and N. Kawada, "Differential absorption lidar at 1.67 μm for remote sensing of methane leakage," Jpn. J. Appl. Phys. **38**, 110–114 (1999).
18. J. Chen, A. Hangauer, R. Strzoda, T. G. Euser, J. S. Y. Chen, M. Scharrer, P. S. J. Russell, and M.-C. Amann, "Sensitivity limits for near-infrared gas sensing with suspended-core PCFs directly coupled with VCSELs," in *Conference on Lasers and Electro-Optics 2010*, OSA Technical Digest (CD) (Optical Society of America, 2010), paper JThB7.
19. G. Cheng, Y. Cao, K. Liu, G. Zhu, G. Wang, and X. Gao, "Photoacoustic measurement of ethane with near-infrared DFB diode laser," J. Spectrosc. **2018**, 9765806 (2018).
20. G. Hancock, C. E. Langley, R. Peverall, G. A. D. Ritchie, and D. Taylor, "Laser-based method and sample handling protocol for measuring breath acetone," Anal. Chem. **86**, 5838–5843 (2014).
21. R. Bauer, T. Legg, D. Mitchell, G. M. H. Flockhart, G. Stewart, W. Johnstone, and M. Lengden, "Miniaturized photoacoustic trace gas sensing using a Raman fiber amplifier," J. Light. Technol. **33**, 3773–3780 (2015).
22. Z. Li, Y. Jung, J. M. O. Daniel, N. Simakov, M. Tokurakawa, P. C. Shardlow, D. Jain, J. K. Sahu, A. M. Heidt, W. A. Clarkson, S. U. Alam, and D. J. Richardson, "Exploiting the short wavelength gain of silica-based thulium-doped fiber amplifiers," Opt. Lett. **41**, 2197–2200 (2016).
23. S. Chen, Y. Jung, S. Alam, D. J. Richardson, R. Sidharthan, D. Ho, S. Yoo, and J. M. O. Daniel, "Ultra-short wavelength operation of thulium-doped fiber amplifiers and lasers," Opt. Express **27**, 36699–36707 (2019).
24. M. Nikodem, A. Khegai, and S. V. Firstov, "Single-frequency bismuth-doped fiber power amplifier at 1651 nm," Laser Phys. Lett. **16**, 115102 (2019).
25. N. K. Thipparapu, A. A. Umnikov, P. Barua, and J. K. Sahu, "Bi-doped fiber amplifier with a flat gain of 25 dB operating in the wavelength band 1320–1360 nm," Opt. Lett. **41**, 1518–1521 (2016).
26. N. K. Thipparapu, Y. Wang, A. A. Umnikov, P. Barua, D. J. Richardson, and J. K. Sahu, "40 dB gain all fiber bismuth-doped amplifier operating in the O-band," Opt. Lett. **44**, 2248–2251 (2019).
27. N. K. Thipparapu, Y. Wang, S. Wang, A. A. Umnikov, P. Barua, and J. K. Sahu, "Bi-doped fiber amplifiers and lasers," Opt. Mater. Express **9**, 2446–2465 (2019).
28. E. M. Dianov, M. A. Mel'kumov, A. V. Shubin, S. V. Firstov, V. F. Khopin, A. N. Gur'yanov, and I. A. Bufetov, "Bismuth-doped fibre amplifier for the range 1300–1340 nm," Quantum Electron. **39**, 1099–1101 (2009).
29. S. Alyshev, A. Kharakhordin, E. Firstova, A. Khegai, M. Melkumov, V. Khopin, A. Lobanov, A. Guryanov, and S. Firstov, "Photostability of laser-active centers in bismuth-doped GeO2-SiO2 glass fibers under pumping at 1550 nm," Opt. Express **27**, 31542–31552 (2019).
30. S. V. Firstov, S. V. Alyshev, K. E. Riumkin, V. F. Khopin, A. N. Guryanov, M. A. Melkumov, and E. M. Dianov, "A 23-dB bismuth-doped optical fiber amplifier for a 1700-nm band," Sci. Rep. **6**, 28939 (2016).
31. A. Yeniay, J.-M. Delavaux, and J. Toulouse, "Spontaneous and stimulated Brillouin scattering gain spectra in optical fibers," J. Lightwave Technol. **20**, 1425–1432 (2002).
32. P. Kluczynski, J. Gustafsson, Å. M. Lindberg, and O. Axner, "Wavelength modulation absorption spectrometry—an extensive scrutiny of the generation of signals," Spectrochim. Acta B Atom. Spectros. **56**, 1277–1354 (2001).
33. P. Kluczynski and O. Axner, "Theoretical description based on Fourier analysis of wavelength-modulation spectrometry in terms of analytical and background signals," Appl. Opt. **38**, 5803–5815 (1999).
34. G. B. Rieker, J. B. Jeffries, and R. K. Hanson, "Calibration-free wavelength-modulation spectroscopy for measurements of gas temperature and concentration in harsh environments," Appl. Opt. **48**, 5546–5560 (2009).
35. L. Tao, K. Sun, M. A. Khan, D. J. Miller, and M. A. Zondlo, "Compact and portable open-path sensor for simultaneous measurements of

atmospheric N2O and CO using a quantum cascade laser," Opt. Express **20**, 28106–28118 (2012).
36. L. S. Rothman, I. E. Gordon, A. Barbe, D. C. Benner, P. F. Bernath, M. Birk, V. Boudon, L. R. Brown, A. Campargue, J.-P. Champion, K. Chance, L. H. Coudert, V. Dana, V. M. Devi, S. Fally, J.-M. Flaud, R. R. Gamache, A. Goldman, D. Jacquemart, I. Kleiner, N. Lacome, W. J. Lafferty, J.-Y. Mandin, S. T. Massie, S. N. Mikhailenko, C. E. Miller, N. Moazzen-Ahmadi, O. V. Naumenko, A. V. Nikitin, J. Orphal, V. I. Perevalov, A. Perrin, A. Predoi-Cross, C. P. Rinsland, M. Rotger, M. Šimečková, M. A. H. Smith, K. Sung, S. A. Tashkun, J. Tennyson, R. A. Toth, A. C. Vandaele, and J. Vander Auwera, "The HITRAN 2008 molecular spectroscopic database," J. Quant. Spectrosc. Radiat. Transfer **110**, 533–572 (2009).
37. K. Ikuta, N. Yoshikane, N. Vasa, Y. Oki, M. Maeda, M. Uchiumi, Y. Tsumura, J. Nakagawa, and N. Kawada, "Differential absorption lidar at 1.67 μm for remote sensing of methane leakage," Jpn. J. Appl. Phys. **38**, 110–114 (1999).
38. T. Milde, M. Hoppe, H. Tatenguem, C. Assmann, W. Schade, and J. Sacher, "Comparison of the spectral excitation behavior of methane according to InP, GaSb, IC, and QC lasers as excitation source by sensor applications," Appl. Opt. **58**, C84–C91 (2019).
39. G. Plant, Y. Chen, and G. Wysocki, "Optical heterodyne-enhanced chirped laser dispersion spectroscopy," Opt. Lett. **42**, 2770–2773 (2017).